

Fourier Transform Infrared and Resonance Raman Studies of the Interaction of Azide with Cytochrome *c* Oxidase from *Paracoccus denitrificans*

Magdalini Vamvouka,[†] Werner Müller,[‡] Bernd Ludwig,[‡] and Constantinos Varotsis^{*,†}

Department of Chemistry, University of Crete, 71409 Iraklion, Crete, Greece, and Institut für Biochemie, Molekulare Genetik, Johann Wolfgang Goethe-Universität, Biozentrum N200, Marie-Curie-Strasse 9, D-60439 Frankfurt/M., Germany

Received: December 2, 1998

The interaction of azide with oxidized cytochrome *c* oxidase from *Paracoccus denitrificans* has been studied by resonance Raman, Fourier transform infrared, and UV–vis spectroscopy. Azide binds in two phases: a high-affinity phase ($K_d = 4.1 \mu\text{M}$) in which it is bound to a nonmetal site near the binuclear center and a low-affinity phase ($K_d = 11.4 \text{ mM}$) in which it is bound as a bridge to the binuclear center. The resonance Raman spectra of the low-affinity phase display one isotope-dependent vibrational mode at 417 cm^{-1} . The FTIR spectra display two isotope-dependent bands at 2038 and 2056 cm^{-1} . We assign the band at 417 cm^{-1} to $\nu(\text{Fe}-\text{N}_3-\text{Cu}_B)$ and the bands at 2038 and 2056 cm^{-1} to $\nu_{\text{as}}(\text{N}_3)$. We observe similar FTIR spectra for the azide complex of bovine heart oxidase and conclude that the binuclear center in this oxidase behaves in a manner analogous to the *P. denitrificans* enzyme. In contrast to mammalian cytochrome *c* oxidase (Li, W.; Palmer, G. *Biochemistry* **1993**, 322, 1833–1843), the low-affinity phase observed in the interaction of azide with the *P. denitrificans* enzyme is not associated with binding of azide to heme *a*. The observation of two FTIR $\nu_{\text{as}}(\text{N}_3)$ modes suggests that the azide ion binds to two different enzyme conformations, both forming bridging complexes with the binuclear center. Comparison of the UV–vis, resonance Raman, and FTIR data of the azide-bound cytochrome *c* aa_3 from *P. denitrificans* and those of azide-bound quinol cytochrome bo_3 suggest significant alterations in the interaction of azide with the oxidized forms of these bacterial oxidases resulting from specific structural differences within their respective heme $a_3-\text{Cu}_B$ and heme $o_3-\text{Cu}_B$ binuclear pockets.

Cytochrome *c* oxidase, one of the terminal oxidases in *Paracoccus denitrificans*, catalyzes the transfer of electrons from reduced cytochrome *c* to molecular oxygen and translocates protons vectorially across the membrane.^{1–7} The redox active centers of the enzyme are two A-type hemes, one low-spin and one high-spin, called heme *a* and heme a_3 , respectively, and two copper centers, Cu_A and Cu_B . It is now well established that heme a_3 and Cu_B form a binuclear center that binds dioxygen, and electrons are transferred to the $a_3-\text{Cu}_B$ center via Cu_A and heme *a*.⁸ Despite intensive research efforts, neither the mechanism of proton pumping nor the redox centers associated with the redox linkage have been identified. It is believed, however, that the proton translocation process is implemented at the binuclear center.⁹ The recently determined high-resolution structures of cytochrome oxidase from bovine^{10a,b} and *P. denitrificans*² have greatly facilitated the elucidation of this mechanism. The crystal structure of *P. denitrificans* obtained in the presence of azide shows no electron density associated with histidine-325, while the crystal structure of the bovine enzyme obtained in the absence of inhibitors clearly exhibits electron density associated with all three nitrogenous ligands of Cu_B .

As a first step in unraveling the origin of the distal ligand exchange¹¹ and putative histidine cycle/shuttle⁹ mechanisms proposed for coupling proton translocation to redox and coordination events in the heme–copper binuclear center, it is

necessary to clarify to what extent the heme and/or the copper ion can alter or expand their coordination spheres. An approach to such an understanding is to study the spectra of the binuclear center with alternate ligands such as carbon monoxide, azide, cyanide, and formate. Cytochrome aa_3 from *P. denitrificans* has been extensively characterized and is accessible for mutagenesis studies.⁵ Comparison of this bacterial aa_3 to other oxidases may increase our understanding of the structural and functional properties of all heme–copper oxidases and should provide ways by which to identify the conserved structural features that are involved in the fundamental functions common to all terminal oxidases.

The Fourier transform infrared (FTIR) technique is a powerful tool to determine the nature of ligand binding in heme proteins. The FTIR spectra of azide bound to bovine cytochrome oxidase were first reported by Yoshikawa and Caughey.¹² These authors identified infrared bands at 2051 and 2039 cm^{-1} and assigned them to the asymmetric stretch of bound azide to a nonmetal site and a Cu_B-N_3 species, respectively. Additional information concerning the properties of the binuclear center upon azide binding was also reported by Tsubaki.¹³ Li and Palmer, however, monitored the N_3 reaction and found that azide binds in two phases: one of high affinity in which it is bound as a bridge to the heme $a_3-\text{Cu}_B$ center and a low-affinity phase in which it displaces one of the axial ligands to heme *a*.¹⁴

In the work presented here, the interaction of azide with the bimetallic heme–copper site of oxidized cytochrome *c* oxidase isolated from *P. denitrificans* has been characterized by resonance Raman (RR), FTIR, and UV–vis spectroscopy. These

* Corresponding author. Fax: 30-81-210951. E-mail: varotsis@cc.uoh.gr.

[†] University of Crete.

[‡] Johann Wolfgang Goethe-Universität.

results have been compared with data on the well-studied cytochrome *c* oxidase from bovine heart. Our results indicate that azide binds in two phases: a high-affinity phase ($K_d = 4.1 \mu\text{M}$) in which it is bound to a nonmetal site near the binuclear center and a low-affinity phase ($K_d = 11.4 \text{ mM}$) in which it is bridged to the binuclear heme a_3 - Cu_B center. The azide-sensitive modes observed at 417 cm^{-1} in the resonance Raman spectra, and at 2056 and 2038 cm^{-1} in the FTIR spectra arise from $\nu(\text{Fe}-\text{N}_3-\text{Cu}_B)$ and $\nu_{\text{as}}(\text{N}_3)$, respectively, of the heme a_3 $\text{Fe}-\text{N}=\text{N}=\text{N}-\text{Cu}_B$ complex. In addition, the high-frequency resonance Raman data show that the heme *a* center of the *P. denitrificans* enzyme is unaffected by high concentrations of azide, suggesting that the low-affinity phase, as opposed to mammalian cytochrome *c* oxidase, is not associated with binding of azide to heme *a*. The observation of two $\nu_{\text{as}}(\text{N}_3)$ modes suggest that azide binds in two different conformational states, both forming bridging complexes with the binuclear center.

Materials and Methods

Cytochrome *c* oxidase (CcO) was isolated from beef hearts by using a modified Hartzell and Beinert preparation¹⁵ and from *P. denitrificans* according to published procedures.⁷ The samples were stored in liquid nitrogen until further use. FTIR spectra were recorded at 2 cm^{-1} resolution with a Bruker Equinox 55 FTIR spectrometer equipped with a liquid nitrogen cooled mercury cadmium telluride detector. Concentrated CcO solutions (120 – $250 \mu\text{M}$) in 50 mM Hepes, 0.3% lauryl maltoside, pH 7.4 , were mixed with small volumes of a sodium azide solution in the same buffer to a final concentration of 20 mM . The protein solution was loaded into a cell with CaF_2 windows and a 0.05 mm spacer. Absorption spectra in the range 1900 – 2100 cm^{-1} were obtained from the difference between the spectra of the CcO–azide complexes and the spectrum of oxidized CcO. The infrared spectrum of CcO in the absence of azide (minus the buffer spectrum) does not exhibit any significant bands over this range. An average of 2100 scans was used for each spectrum. Optical absorption spectra were recorded in the FTIR cell before and after FTIR measurements in order to assess sample stability with a Perkin-Elmer Lambda 20 UV–visible spectrometer. Resonance Raman spectra were obtained from 30 – $40 \mu\text{M}$ samples, pH 7.6 , in a cylindrical quartz spinning cell maintained at 3 – 5°C by a stream of cold nitrogen gas. The Raman spectra were acquired by using a SPEX 1877 triplemate with an EG&G (model 1530-CUV-1024S) CCD detector. A Coherent Innova K-90 krypton ion laser was used to provide the excitation wavelength of 413.1 nm . A Coherent 590 dye laser connected with a Coherent Innova 200 argon laser was used to provide the excitation wavelength of 427 nm . The power incident on the oxidase samples was typically 8 – 10 mW . Sodium azide (NaN_3) was obtained from Aldrich and $\text{Na}^{15}\text{N}^{14}\text{N}^{14}\text{N}$ from Cambridge Isotopes.

Results and Discussion

Figure 1 shows the absorption spectra of oxidized CcO (Figure 1A), the azide-bound CcO (Figure 1B), and the difference spectra of azide-bound CcO minus oxidized CcO. The difference spectra are characterized by two series of absorbance changes. The overall shape of the difference spectra presented here for *P. denitrificans* is similar to those reported for the bovine enzyme by Li and Palmer;¹⁴ in contrast to the bovine enzyme, the Soret maximum of the *P. denitrificans* enzyme in the presence of 5 mM azide is red-shifted and occurs at 430 nm . Titration of *P. denitrificans* with azide concentrations

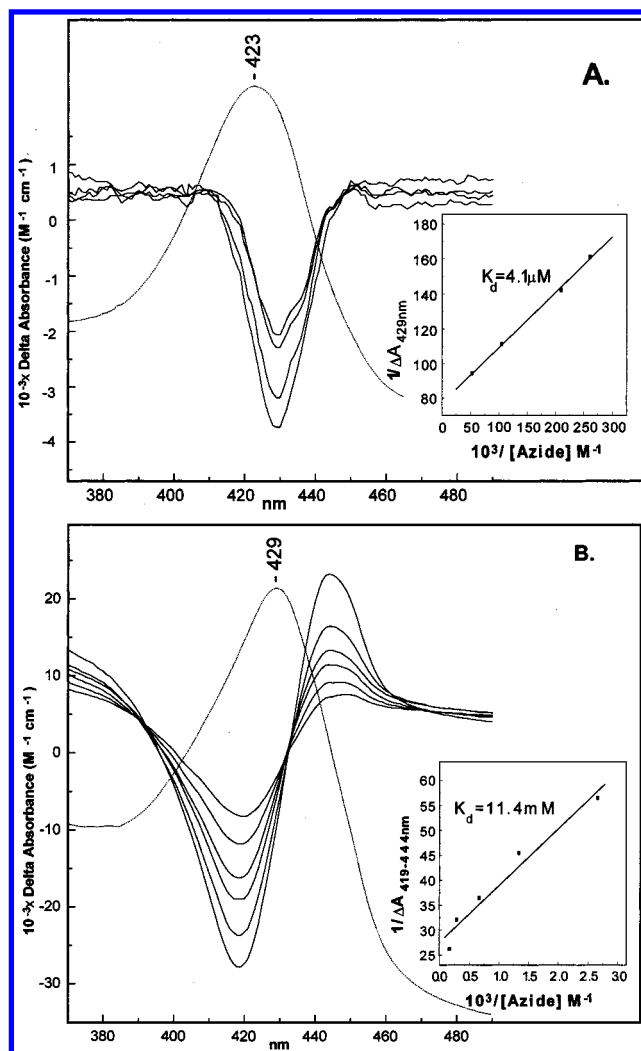


Figure 1. Optical absorption spectra of oxidized *Paracoccus denitrificans* CcO (Figure 1A), the azide-bound CcO (Figure 1B), and the difference spectra of CcO–azide minus CcO. All spectra were recorded in a 0.5 cm path length at 25°C . The enzyme was diluted to a final concentration of $5.5 \mu\text{M}$ in 50 mM Hepes and 0.3% dodecyl β -D-maltoside at pH 7.4 . Ten minutes after each addition, a new difference spectrum was taken. (A) The stoichiometry of $[\text{aa}_3]:[\text{N}_3]$ was $1:0.8$, $1:1.2$, $1:2$, and $1:4$. The inset shows a double-reciprocal plot of the absorbance decrease at 429 nm versus azide concentration yielding a $K_d = 4.1 \mu\text{M}$. (B) The stoichiometry of $[\text{aa}_3]:[\text{N}_3]$ was $1:80$, $1:160$, $1:320$, $1:640$, $1:1200$, and $1:2200$. The inset shows a double-reciprocal plot of 419 – 444 nm versus total azide concentration yielding a $K_d = 11.4 \text{ mM}$.

below 0.4 mM causes small decreases in the Soret absorbance. The difference spectra (Figure 1A) exhibit a trough at 429 nm , and a zero crossing at 410 nm . A double-reciprocal plot of ΔA_{429} versus azide concentration is linear (Figure 1A, inset) and yields a $K_d = 4.1 \mu\text{M}$ at pH 7.4 . We call this the high-affinity phase. Upon a further increase in azide concentration the observed difference spectra, shown in Figure 1B, exhibit a minimum at 419 nm and a maximum at 444 nm . The double-reciprocal plot of $\Delta A_{419-444}$ versus azide concentration is displayed in the inset and yields a $K_d = 11.4 \text{ mM}$. We refer to this reaction as the low-affinity phase. Moreover, there were no spectral changes in the α -band during the high- and low-affinity phases.

The small spectral changes and the magnitude of the dissociation constant ($K_d = 4.1 \mu\text{M}$) for azide binding to CcO from *P. denitrificans* suggest that this corresponds to the high-affinity phase ($K_d = 64 \mu\text{M}$) of azide binding to bovine CcO found by Li and Palmer.¹⁴ Our measured dissociation constant

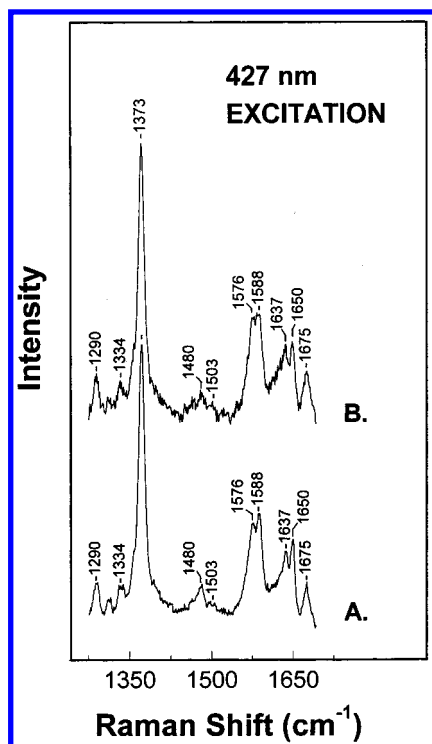


Figure 2. High-frequency resonance Raman spectra of cytochrome *aa*₃ from *P. denitrificans*: (A) oxidized cytochrome *aa*₃; (B) oxidized + 20 mM ¹⁴N₃ (low-affinity). The exciting laser frequency was 427 nm.

of 4.1 μ M obtained at pH 7.4 is almost 15 times smaller than those obtained at pH 8.0 by Li et al.¹⁴ and Vygodina et al.,¹⁶ and close to the value of 20 μ M obtained at pH 7.2 by Wever et al.¹⁷ for the bovine enzyme, and to that of 17 μ M found by Little et al.¹⁸ for cytochrome *bo*₃. The difference in the dissociation constants between *P. denitrificans* and mammalian CcO may well be due to intrinsic differences between these two enzymes as well as a choice of experimental conditions.

The electronic spectra of the *aa*₃-N₃ complexes studied here are relatively insensitive to the conformation of the bound azide or to changes in the *a*₃-Cu_B pocket. As part of our attempt to obtain further insights into the interaction of azide with the *P. denitrificans* enzyme, we have obtained the resonance Raman and FTIR spectra of the azide-bound enzyme.

Figure 2A shows the high-frequency resonance Raman spectrum of fully oxidized *aa*₃, and that of the azide-bound enzyme is shown in Figure 2B. With 427 nm excitation, the contribution of heme *a* to the resonance Raman spectrum of resting enzyme is emphasized because of the relative positions of the Soret maxima of heme *a* at 427 nm and heme *a*₃ at 416 nm. In the spectrum of the resting enzyme, the oxidation state marker is at 1373 cm⁻¹, establishing that both hemes are in the ferric state. The core expansion region shows two vibrations at 1576 cm⁻¹ (high spin heme *a*₃³⁺) and 1588 cm⁻¹ (low-spin heme *a*³⁺). The 1637 cm⁻¹ mode arises from ν_{10} of heme *a*₃³⁺. The 1650 and 1675 cm⁻¹ modes are the C=O stretching vibration of the formyl groups (-CHO) of heme *a*³⁺ and heme *a*₃³⁺, respectively. The frequencies of these modes are similar to those that occur in the mammalian enzyme.¹⁹ Addition of azide (20 mM; low-affinity phase) to oxidized enzyme causes neither frequency nor intensity changes in the RR bands of heme *a*; the ν_2 of heme *a*₃ at 1576 cm⁻¹ has gained intensity. This indicates that there are not any changes in the heme *a* environment and that heme *a* remains six-coordinate low-spin and heme *a*₃ six-coordinate high-spin.

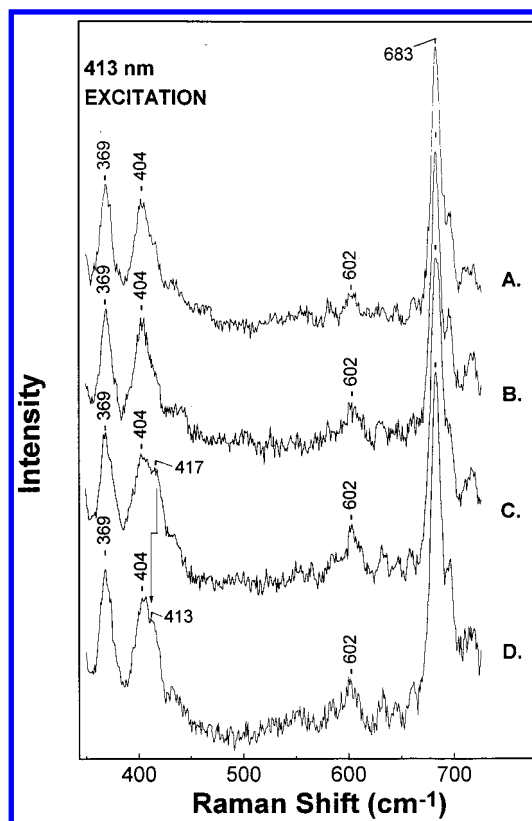


Figure 3. Low-frequency resonance Raman spectra of cytochrome *aa*₃ from *P. denitrificans*: (A) oxidized cytochrome *aa*₃; (B) oxidized + 100 μ M ¹⁴N₃ (high-affinity); (C) oxidized + 20 mM ¹⁴N₃ (low-affinity); (D) oxidized + 20 mM ¹⁵N¹⁴N₂ (low-affinity). The exciting laser frequency was 413.1 nm.

Figure 3 shows the low-frequency RR spectra of (A) oxidized, (B) oxidized + 100 μ M ¹⁴N₃ (high-affinity), (C) oxidized + 20 mM ¹⁴N₃ (low-affinity), (D) oxidized + 20 mM ¹⁴N₂¹⁵N (low-affinity) cytochrome *aa*₃ obtained by using the 413.1 nm excitation frequency, in which resonances of both hemes are enhanced. The principal bands seen in Figure 3A located at 369, 404, and 683 cm⁻¹ have contributions from both heme *a*₃ and heme *a*. Spectrum B (¹⁴N₃, high-affinity) is similar to spectrum A. This observation suggests that neither the heme *a*₃ nor the heme *a* environment are affected during the high-affinity phase. Spectrum C is similar to spectra A and B with the exception that a new mode is observed at 417 cm⁻¹. Spectrum D shows that the 417 cm⁻¹ mode in the ¹⁴N₃ spectrum is downshifted to 413 cm⁻¹ when the experiment is repeated with ¹⁵N₂¹⁴N. The 4 cm⁻¹ isotope shift of this mode and its frequency allows us to assign it as the heme *a*₃ Fe-N₃ stretching vibration. The frequency of this mode is close to that reported for Mb-N₃ and Hb-N₃.^{20a-c} The 4 cm⁻¹ isotope shift we detect, however, is small when compared to the 7 cm⁻¹ shift observed in Mb-N₃. This suggests that Cu_B has a direct interaction with the bound to heme *a*₃ azide and that the azide molecule is bridged between heme *a*₃ and Cu_B.

The FTIR spectrum of ¹⁴N₃-bound *P. denitrificans aa*₃ (trace A in Figure 4) obtained at neutral pH exhibits bands at 2056 and 2038 cm⁻¹, both of which display azide isotopic sensitivity by shifting to 2043/2037 and 2024 cm⁻¹, respectively, in the ¹⁵N¹⁴N¹⁴N derivative (trace B). Comparison of spectrum A with spectrum C of Figure 4 shows that similar results are obtained for azide-bound *P. denitrificans* and mammalian *aa*₃ oxidase. The frequencies of these azide-sensitive modes are all very close to those that have been reported for the azide adducts of mammalian cytochrome *c* oxidase.¹²⁻¹⁴ There are some clear

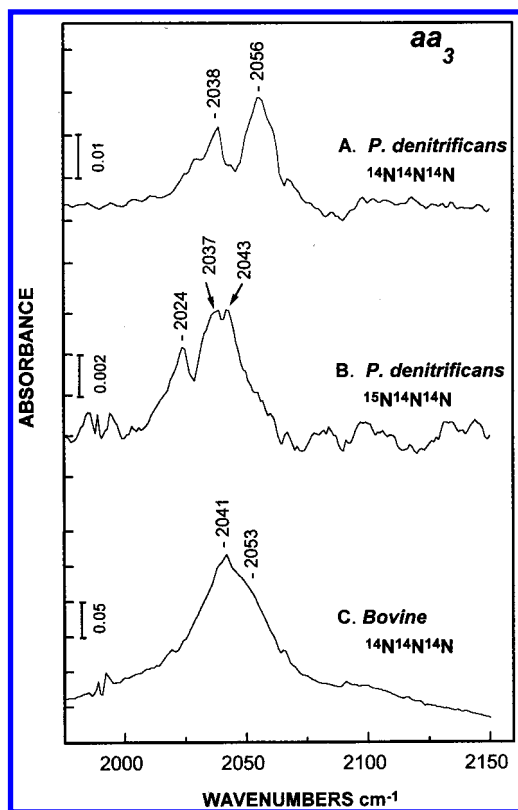


Figure 4. FTIR spectra of oxidized CcO from *P. denitrificans* (spectra A and B) and bovine (spectrum C) in the presence of $^{14}\text{N}_3$ and $^{15}\text{N}^{14}\text{N}^{14}\text{N}$. The final concentration of azide was 20 mM (low-affinity phase).

differences, however. The 2056- and 2038 cm^{-1} modes are 3–5 cm^{-1} higher and 2–3 cm^{-1} lower, respectively, in *P. denitrificans* compared to mammalian oxidase, and the splitting of the 2051 cm^{-1} mode obtained with ^{15}N is of the order of 9 cm^{-1} for the mammalian enzyme while the analogous splitting found in *P. denitrificans* is 6 cm^{-1} . In cytochrome bo_3 Tsubaki et al.²¹ suggested that the 2041 cm^{-1} mode observed in their FTIR spectra arises from the asymmetric stretch of the bridged between heme o_3 and Cu_B azide molecule. Thus the small frequency differences between the azide-isotope-sensitive modes in *P. denitrificans* and mammalian cytochrome aa_3 and cytochrome bo_3 do indicate that the binuclear site of the *P. denitrificans* enzyme, while similar, is not completely identical to mammalian cytochrome aa_3 and cytochrome bo_3 .

A number of chemically interesting structures have been suggested for azide-bound bovine CcO^{12–14} and cytochrome bo_3 .²¹ Yoshikawa and Caughey¹² interpreted their optical and FTIR data to indicate azide binding associated within the protein moiety near the binuclear site ($\nu_{\text{asym}} = 2051 \text{ cm}^{-1}$) and to Cu_B ($\nu_{\text{asym}} = 2038 \text{ cm}^{-1}$). This interpretation was challenged by Tsubaki¹³ who, using data obtained from FTIR spectroscopy, argued that the 2051 cm^{-1} mode arises from a bridging structure between a_3 and Cu_B and the 2039 cm^{-1} mode is from a ferric a_3 -azide high-spin species. The belief that the 2039 cm^{-1} mode is associated with a $a_3\text{--N}_3$ or a $\text{Cu}_B\text{--N}_3$ species was cautiously endorsed by Li and Palmer,¹⁴ who interpreted the FTIR, EPR, and MCD data to assign this mode to azide bound to heme *a*. In addition, the same authors observed a 9 cm^{-1} splitting of the 2051 cm^{-1} vibration when the experiment was repeated in the presence of $^{15}\text{N}^{14}\text{N}^{14}\text{N}$. Although the FTIR data suggested that azide binds as a terminal ligand to a metal, most probably to Cu_B , they concluded that the 2051 cm^{-1} vibration was due to the bridging azide between heme a_3 and Cu_B . This interpreta-

tion largely rested on the observation that both the 2051 and 2039 cm^{-1} modes could be replaced with a minimum amount of cyanide, producing the $a_3\text{--C}\equiv\text{N--Cu}_B$ bridging structure characterized by the 2152 cm^{-1} mode, and therefore the azide ion must occupy the same or overlapping site with this bridging cyanide. Unfortunately, these three studies have failed to agree on the mode of azide binding to bovine cytochrome *c* oxidase.

The crystal structure of *P. denitrificans* in the presence of 0.1% azide showed that heme *a* is a bis-histidine-coordinated low-spin species.² In addition, the RR data presented here suggest that the heme *a* environment is unaffected by the addition of N_3 to the enzyme. Therefore, neither the 2056 cm^{-1} nor the 2038 cm^{-1} modes we observe in *P. denitrificans* are associated with azide binding to heme *a*. The most reasonable assignment of the 2056 cm^{-1} mode is that it arises from a heme $a_3\text{Fe--N}_3\text{--Cu}_B$ complex. For such a bridging structure, the 2056 cm^{-1} mode should split in the $^{15}\text{N}_3$ experiment due to a difference in the N–N asymmetric stretch arising from the differences in the $\text{Cu}_B\text{--N}$ and Fe--N bonding. The observed splitting of this mode in the FTIR data supports our assignment. On the other hand, the 2038 cm^{-1} mode did not show any detectable splitting upon replacement with $^{15}\text{N}^{14}\text{N}^{14}\text{N}$, indicating that the strengths of the two internal N=N bonds of azide were very similar to each other. The 2038 cm^{-1} frequency is close to 2042 cm^{-1} observed for Mb– N_3 .^{22–25} Despite the similarity in those two frequencies, we propose that the azide molecule is not terminally bound to heme a_3 but it binds in two distinct conformations within the $a_3\text{--Cu}_B$ center (see below). We suggest that the first adduct arises from a conformation that is described by the 417 cm^{-1} /2056 cm^{-1} modes and the second by the 417 cm^{-1} /2038 cm^{-1} modes. Such different conformational states have been proposed to occur in the mammalian–CcO–azide complex by Tsubaki.¹³ Additional asymmetric azide bands have also been assigned in the FTIR spectra of elephant Mb and horse heart Mb.^{24,25} In elephant Mb, the presence of an additional covalent band at 2041 cm^{-1} and an additional ionic band at 2054 cm^{-1} are proposed to arise from two different heme– N_3 conformations that affect the asymmetric azide stretch. Thus the large difference in frequency between the 2056 and 2038 cm^{-1} modes observed in the *P. denitrificans* enzyme could be explained by an increase of the metal–N bond order in conjunction with a decrease in the bond order of the N=N bond in the case of the 2038 cm^{-1} mode. The angle between either the heme a_3 iron and/or the Cu_B and the N1 and N2 atoms of the azide molecule can also influence the frequency of the asymmetric azide stretch. If azide is coordinated to heme a_3 , trans to the proximal histidine and not bridging to Cu_B , one would expect heme a_3 to acquire a low-spin character. There is no evidence for any new low-spin species from the RR data. Thus, neither the 2056 cm^{-1} nor the 2038 cm^{-1} modes could arise from azide binding terminally to heme a_3 .

Combining the results above with those observed for the mammalian CcO and cytochrome bo_3 complexes yields following points. First, unlike the reaction of azide with mammalian CcO, the low-affinity phase observed in the reaction of azide with the *P. denitrificans* enzyme is not associated with binding of azide to heme *a* but it involves the binuclear heme $a_3\text{--Cu}_B$ center. Second, comparison of the K_d values and FTIR data of the azide-bound cytochrome bo_3 and cytochrome aa_3 from *P. denitrificans* complexes reveals that there are quantitative differences in the kinetics of azide binding, and in the structure of the heme $o_3\text{--Cu}_B$ and heme $a_3\text{--Cu}_B$ binuclear pockets upon azide binding. Such differences can be attributed to changes in the position of Cu_B . Our interpretation that azide binds as a

bridging ligand between heme a_3 and Cu_B is consistent with the recent structural information about the binuclear center of mammalian cytochrome aa_3 oxidase.^{10b} Interestingly, the crystal structure of the *P. denitrificans* enzyme in the presence of azide showed no electron density as histidine-325, suggesting that binding of azide causes H325 to be displaced. It is noteworthy that Puustinen et al.²⁶ recently suggested that the binding of CO to Cu_B from the photodissociated heme o_3 -CO adduct induced a change in the Lewis acidity of Cu_B or the displacement of a Cu_B ligand. We expect that the phenomena observed in the coordination dynamics of azide are representative of the behavior of other ligands including CO and, most importantly, O_2 . In this case, the properties of the structurally rearranged Cu_B in acting as an intermediate binding site for ligands entering and leaving the site for O_2 reduction have profound functional significance. Considering the reported role of Cu_B in the functional dynamics of the enzyme, it is especially important to delineate the properties of this center in the catalytic process under physiological conditions.

Acknowledgment. This work was supported by Alexander von Humboldt-Stiftung, DFG (SFB 472), Fonds der Chemischen Industrie, and PENED-95. We are indebted to Prof. G. Babcock for the use of the LASER facility at M.S.U.

References and Notes

- (1) Babcock, G. T.; Wikström, M. *Nature* **1992**, *356*, 301–309.
- (2) Iwata, S.; Ostermeier, C.; Ludwig, B.; Michel, H. *Nature* **1995**, *376*, 660–669.
- (3) Ludwig, B. *FEMS Microbiol. Rev.* **1987**, *46*, 41–56.
- (4) Gennis, R. B.; Trumpower, B. L. *Annu. Rev. Biochem.* **1994**, *63*, 675–716.
- (5) Steinrück, P.; Gerhus, E.; Ludwig, B. *J. Biol. Chem.* **1991**, *266*, 7676–7681.
- (6) Capaldi, R. A. *Annu. Rev. Biochem.* **1990**, *59*, 569–596.
- (7) Hendler, R. W.; Pardhasaradhi, K.; Reynafarje, B.; Ludwig, B. *Biophys. J.* **1991**, *60*, 415–423.
- (8) Einarsson, O. *Biochim. Biophys. Acta* **1995**, *1229*, 129–147.
- (9) Morgan, J. E.; Verkhovsky, M. I.; Wikström, M. *J. Bioenerg. Biomembr.* **1994**, *26*, 599–608.
- (10) (a) Tsukihara, T.; Aoyama, H.; Yamashita, E.; Tomizaki, T.; Tamaguchi, H.; Shinzawa-Itoh, K.; Nakashina, R.; Yaono, R.; Yoshikawa, S. *Science* **1996**, *272*, 1136–1144. (b) Yoshikawa, S.; Shinzawa-Itoh, K.; Nakashina, R.; Yaono, R.; Yamashita, E.; Inoue, N.; Yao, M.; Fei, M. J.; Libeu, C. P.; Mizushima, T.; Yamaguchi, H.; Tomizaki, T.; Tsukihara, T. *Science* **1998**, *280*, 1723–1729.
- (11) Woodruff, W. H.; Einarsson, O.; Dyer, R. B.; Bagley, K. A.; Palmer, G.; Atherton, S. J.; Goldbeck, R. A.; Dawes, T. D.; Kliger, D. S. *Proc. Natl. Acad. Sci. U.S.A.* **1991**, *88*, 2588–2592.
- (12) Yoshikawa, S.; Caughey, W. S. *J. Biol. Chem.* **1992**, *267*, 9757–9766.
- (13) Tsubaki, M. *Biochemistry* **1993**, *32*, 174–182.
- (14) Li, W.; Palmer, G. *Biochemistry* **1993**, *32*, 1833–1843.
- (15) Hartzell, R.; Beinert, H. *Biochim. Biophys. Acta* **1974**, *368*, 318–338.
- (16) Vygoda, T. V.; Konstantinov, A. A. *Biol. Membr.* **1985**, *2*, 861–869.
- (17) Wever, R.; Muijsers, A. O.; Van Gelder, B. F.; Bakker, E. P.; Van Buuren, K. J. *Biochim. Biophys. Acta* **1973**, *325*, 1–7.
- (18) Little, R. H.; Cheesman, M. R.; Thomson, A. J.; Greenwood, C.; Watmough, N. J. *Biochemistry* **1996**, *35*, 13780–13787.
- (19) Babcock, G. T. In *Biological Applications of Raman Spectroscopy*; Spiro, T. G., Ed.; Wiley: New York, 1988; Vol. 3, p 293.
- (20) (a) Asher, S. A.; Vickery, L. E.; Schuster, T. M.; Sauer, K. *Biochemistry* **1977**, *16*, 5849–5855. (b) Asher, S. A.; Schuster, T. M. *Biochemistry* **1979**, *18*, 5377–5382. (c) Desbois, A.; Lutz, M.; Banerjee, R. *Biochemistry* **1979**, *18*, 1510–1515. (d) Tsubaki, M.; Srivastava, R. B.; Yu, N.-T. *Biochemistry* **1979**, *18*, 946–952. (e) Czernuszewicz, R. S.; Wagner, W.-D.; Ray, G. B.; Nakamoto, K. *J. Mol. Struct.* **1991**, *242*, 99–117.
- (21) Tsubaki, M.; Mogi, T.; Anraku, Y.; Hori, H. *Biochemistry* **1993**, *32*, 6065–6072.
- (22) McCoy, S.; Caughey, W. S. *Biochemistry* **1970**, *9*, 2387–2392.
- (23) Alben, J. O.; Fager, L. Y. *Biochemistry* **1972**, *11*, 842–847.
- (24) Bormett, R. W.; Asher, S. A.; Larkin, P. J.; Gustafson, W. G.; Ragunathan, N.; Freedman, T. B.; Nafie, L. A.; Balasubramanian, S.; Boxer, S. G.; Yu, N.-T.; Gersonde, K.; Noble, R. W.; Springer, B. A.; Sligar, S. G. *J. Am. Chem. Soc.* **1992**, *114*, 6864–6867.
- (25) Bogumil, R.; Hunter, C. L.; Maurus, R.; Tang, H.-L.; Lee, H.; Lloyd, E.; Brayer, G. D.; Smith, M.; Mauk, A. G. *Biochemistry* **1994**, *33*, 7600–7608.
- (26) Puustinen, A.; Baily, J. A.; Dyer, R. B.; Mecklenburg, S. L.; Wikström, M.; Woodruff, W. H. *Biochemistry* **1997**, *36*, 13195–13200.